ACCEPTED VERSION

https://link.springer.com/article/10.1007/s11044-017-9587-2

About this article

Check for updates

Cite this article as:
Bélaise, C., Dal Maso, F., Michaud, B. et al. Multibody Syst Dyn (2017). https://doi.org/10.1007/s11044-017-9587-2

DOI
https://doi.org/10.1007/s11044-017-9587-2

Publisher Name
Springer Netherlands

Print ISSN
1384-5640

Online ISSN
1573-272X

About this journal

Reprints and Permissions

An EMG-marker tracking optimisation method for estimating muscle forces

Colombe Bélaise[1,2], Fabien Dal Maso[1,2], Benjamin Michaud[1,2], Katja Mombaur[3], Mickaël Begon[1,2]

[1]*Laboratory of Simulation and Modelisation of Movement, Université de Montréal, QC, CANADA*

[2]*Sainte-Justine Hospital Research Center, Montreal, QC, CANADA*

[3]*Interdisciplinary Center for Scientific Computing (IWR), University of Heidelberg, GERMANY*

colombe.belaise@umontreal.ca

fabien.dalmaso@gmail.com

benjamin.michaud@umontreal.ca

katja.mombaur@iwr.uni-heidelberg.de

mickael.begon@umontreal.ca

Corresponding author: C. Bélaise

Laboratoire de Simulation et Modélisation du Mouvement

Université de Montréal – Campus de Laval

1700, rue Jacques-Tétreault

H7N 0B6 Laval, QC – Canada.

Tel: +1 514-343-6111 #88111

Fax: +1 514-343-2155

Abstract Existing algorithms for estimating muscle forces mainly use least-activation criteria that do not necessarily lead to physiologically consistent results. Our objective was to assess an innovative forward dynamics-based optimisation, assisted by both electromyography (EMG) and marker tracking, for estimating the upper-limb muscle forces. A reference movement was generated and EMG was simulated to reproduce the desired joint kinematics. Random noise was added to both simulated EMG and marker trajectories in order to create 30 trials. Then, muscle forces were estimated using: (1) the innovative EMG-marker tracking forward optimisation; (2) a marker tracking forward optimisation with a least-excitation criterion; (3) and static optimisation with a least-activation criterion. Approaches (1) and (2) were solved using a direct multiple shooting algorithm. Finally, reference and estimated joint angles and muscle forces for the three optimisations were statistically compared using root mean square errors (RMSe), biases and statistical parametric mapping. The joint angles RMSe were qualitatively similar across the three optimisations: (1) 1.63 ± 0.51°; (2) 2.02 ± 0.64°; (3) 0.79 ± 0.38°. However, the muscle forces RMSe for the EMG-marker tracking optimisation (20.39 ± 13.24 N) was about seven times smaller than those resulting from the marker tracking (124.22 ± 118.22 N) and static (148.15 ± 94.01 N) optimisations. The originality of this novel approach was to closely track both simulated EMG and marker trajectories in the same objective-function, using forward dynamics. Therefore, the presented EMG-marker tracking optimisation led to accurate muscle forces estimations.

Keywords *Muscle forces; Musculoskeletal model; Forward dynamics; Electromyography; Direct multiple shooting.*

1. Introduction

Knowledge of muscle contribution to joint torques is necessary to determine postures and movement techniques that would be more likely to cause pain and/or injuries. As invasive methods to measure muscle forces are not applicable in clinical settings, computer musculoskeletal models were developed to estimate them [1]. A significant challenge is the musculoskeletal redundancy [2]; for example, nine muscles cross the glenohumeral joint, which has *only* three degrees-of-freedom in rotation. State-of-the-art methods for solving such underdetermined problems are therefore based on optimisation, which is usually paired with muscle models [3].

Static optimisation – an inverse dynamics-based algorithm combined with a least-activation criterion [4] – is extensively used for its low computational cost and ease of implementation [5]. It proved to be acceptable to estimate lower-limb muscle forces during locomotion-related tasks that do not require lots of co-contraction in able-bodied participants [6-8]. By contrast, at the shoulder joint, stability is partly ensured by the antagonistic efforts of the rotator cuff and deltoid muscles [9-11]. Since muscle co-contraction is not easily predicted using a least-activation/excitation criterion [12], the latter may not be suitable for estimating shoulder muscle forces. Another drawback of inverse dynamics-based algorithms is that they fail to account for the activation dynamics [13]. Thus, unrealistic variations of muscle forces might happen from one instant to another [14]. Conversely, forward dynamics-based algorithms address this non-continuity issue by accounting for the activation dynamics and by solving the system equations forward in time [14]. Muscle excitations are, in fact, iteratively optimised to track kinematics and/or contact forces [13, 15, 16]. However, their major shortcoming is their high convergence time (*e.g.*, 80-160 h with the simulated annealing algorithm [16]), related to the difficulty to find a solution. By developing the computed muscle control algorithm, Thelen and Anderson (2006) [17] addressed this convergence speed issue. Nevertheless, this algorithm remains dependent on static optimisation results [17] for which some weaknesses were aforementioned. Finally, direct collocation [18-21] and direct multiple shooting algorithms

[22-24] have proven their efficiency to solve forward problems in a timely manner, which may offer an attractive alternative to estimate muscle forces.

Whether inverse or forward-dynamic based optimisations, existing algorithms share a common limitation which comes from their objective-function. In fact, experimental electromyography (EMG) is not included within the optimisation process, but often used as validation [12, 16, 25, 26]. Yet, although experimental EMG is known to be affected by various types of noises [27], it explicitly reflects the actual muscle activity. Hybrid EMG-driven algorithms appear to be more convincing, since EMG is used in a feed-forward fashion to calculate joint torques, which are compared to the joint torques obtained from inverse dynamics [28, 29]. However, like any inverse dynamic-based algorithm, hybrid approaches heavily rely on the recording accuracy of kinematics. Indeed, since marker trajectories are affected by soft tissue artefacts (*e.g.*, up to 8.7 cm on the scapula [30, 31]), joint torques are subjected to errors which affect muscle forces estimations [32-34].

Since kinematic and EMG data are both prone to measurement errors [27, 28], our objective was to develop an innovative forward dynamics-based optimisation to estimate muscle forces by tracking both simulated EMG and marker trajectories, using a direct multiple shooting algorithm. To the best of our knowledge, no previous study has tracked both EMG and marker trajectories in the same objective-function for the estimation of muscle forces. We hypothesized that combining the two sources of information may help improve the optimal solution. The proposed method accuracy was assessed and compared to two commonly used static and dynamic optimisations combined with a least-activation/excitation criterion. The term ‘muscle excitations’ was used to refer to ‘simulated EMG’.

2. Methods

2.1 Upper-limb musculoskeletal model

A three-dimensional upper-limb model was created from the musculoskeletal modeling package developed in our laboratory (S2M Dynamic Library), based on the Rigid Body Dynamic Library [35]. The kinematic model consisted of eight rigid segments, namely: the trunk and the right clavicle, scapula, humerus, radius, ulna and hand (**Fig. 1**). Four joints were defined: the sternoclavicular (1 DOF: anterior/posterior rotation), acromioclavicular (1 DOF: anterior/posterior tilting), glenohumeral (3 DOFs: flexion, abduction, axial rotation) and elbow (1 DOF: flexion/extension). Four markers were modelled on each segment for a total of 28 markers (no marker was placed on the spine) (**Fig. 1**).

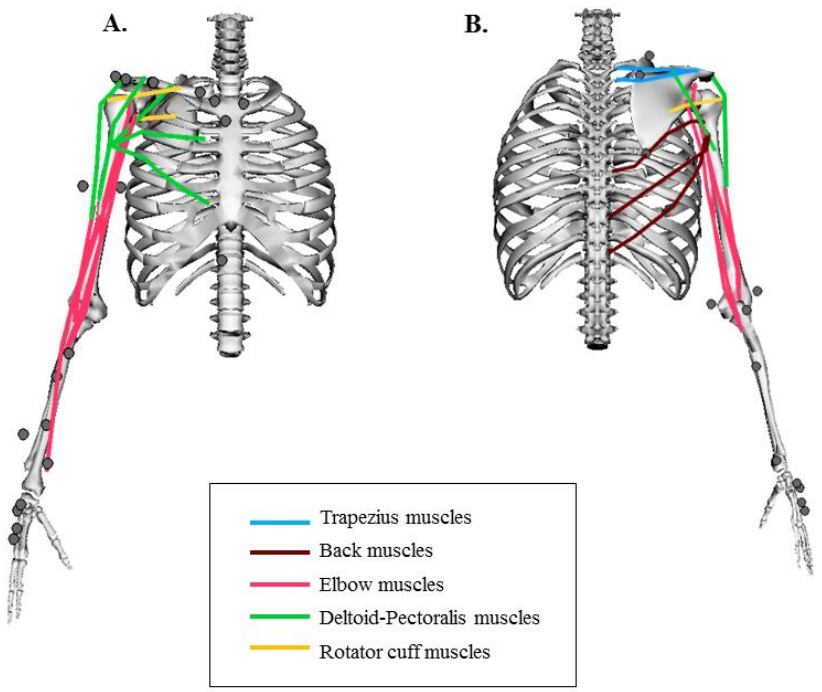

Fig. 1 Anterior (A) and posterior (B) views of the right upper-limb musculoskeletal model derived from the S2M Dynamic Library. Colored lines and dark-circled dots represent the 20 Hill-type muscle lines of action and the 28 markers, respectively

The upper-limb model was driven by 20 Hill-type muscle lines of action (**Table 1**). Their geometry (origin/insertion sites and via points) and properties (optimal length, maximal

force, tendon slack length, pennation angle, physical cross sectional areas and maximal velocity) were defined based on the model of Holzbaur et al. (2005) [36], except for the trapezius [37]. The force produced by each line of action was estimated using a three-elements Hill-type muscle model, with generic force-length, force-velocity and parallel passive elastic force-length equations [29, 38]. The following set of first-order differential equations (ODE) governed the muscle activation dynamics [39]:

$$\dot{\mathbf{a}}(t, \mathbf{e}(t), \mathbf{a}(t)) = \begin{cases} \dfrac{\big(\mathbf{e}(t) - \mathbf{a}(t)\big)}{t_{act}(0.5 + 1.5\,\mathbf{a}(t))}, & \mathbf{e}(t) > \mathbf{a}(t) \quad (1a) \\ \dfrac{\mathbf{e}(t) - \mathbf{a}(t)}{t_{deact}}(0.5 + 1.5\,\mathbf{a}(t)), & \mathbf{e}(t) \le \mathbf{a}(t) \quad (1b) \end{cases}$$

where $\mathbf{e}(t)$ and $\mathbf{a}(t)$ are the excitations and activations, respectively, at time t. Time constants t_{act} and t_{deact} (for activation and deactivation) were set at 10 and 40 ms, respectively [39]. Muscle forces $\mathbf{F_{mus}}$ were calculated from muscle activations $\mathbf{a}$, maximal isometric forces $\mathbf{F^0_{mus}}$, muscle lengths $\boldsymbol{\ell}_{\mathbf{mus}}$ and lengthening velocities $\boldsymbol{v}_{\mathbf{mus}}$ (that derived from the joint generalised positions and velocities $\mathbf{q}$ and $\dot{\mathbf{q}}$) and the generic force-length-velocity relation f, so that:

$$\mathbf{F_{mus}}(\mathbf{q}, \dot{\mathbf{q}}, \mathbf{a}) = \mathbf{a} \cdot f(\mathbf{F^0_{mus}}, \boldsymbol{\ell}_{\mathbf{mus}}, \boldsymbol{v}_{\mathbf{mus}}), \quad (2)$$

Hence, net joint torques $\boldsymbol{\tau}_{\mathbf{mus}}$ due to muscle forces were expressed as follows:

$$\boldsymbol{\tau}_{\mathbf{mus}}(\mathbf{q}, \dot{\mathbf{q}}, \mathbf{a}) = -\,\boldsymbol{\mathcal{J}}(\boldsymbol{\ell}_{\mathbf{mus}})\,\mathbf{F_{mus}}(\mathbf{q}, \dot{\mathbf{q}}, \mathbf{a}), \quad (3)$$

where $\boldsymbol{\mathcal{J}}(\boldsymbol{\ell}_{\mathbf{mus}}) = \frac{\partial \boldsymbol{\ell}_{\mathbf{mus}}}{\partial \mathbf{q}}$ is the Jacobian matrix of the muscle lengths $\boldsymbol{\ell}_{\mathbf{mus}}$. Thus, in the forward-dynamic process, the joint generalised accelerations $\ddot{\mathbf{q}}$ of the model were written as:

$$\ddot{\mathbf{q}} = \boldsymbol{\mathcal{M}}(\mathbf{q})^{-1}\big(\boldsymbol{\tau}_{\mathbf{mus}}(\mathbf{q}, \dot{\mathbf{q}}, \mathbf{a}) - \mathbf{N}(\mathbf{q}, \dot{\mathbf{q}})\dot{\mathbf{q}} - \mathbf{G}(\mathbf{q})\big), \quad (4)$$

where $\boldsymbol{\mathcal{M}}$ is the mass matrix; $\mathbf{N}$ is the nonlinear vector containing centrifugal and Coriolis effects and $\mathbf{G}$ represents the effects of gravity.

Please insert Table 1 here

2.2 Two simulated datasets

The muscle excitations of a one-second noise-free reference movement (kinematics described in **Appendix A**) were obtained by using a direct multiple shooting algorithm implemented in the MUSCOD-II software [23]. Muscle excitations were discretized into a piecewise constant representation on 30 subintervals, *i.e.* 31 nodes (**Fig. 2**). The joint state angles (**q**) at each node were constrained to follow the noise-free reference joint kinematics (**Appendix A**). The excitations initial guess was set at 0.05 for all the muscles at each node.

A second set of muscle excitations was generated with more co-contraction. Thus, the optimisation process was repeated, in which the excitations of five arbitrary-chosen muscles (PEC ribs, LAT ili., TRI med., DELT mid. and SUP muscles) were bounded between 0.3 and 0.95 to enforce co-contraction of their antagonist muscles. The excitations initial guess was set at 0.3 for these five muscles and at 0.05 for the other muscles.

Two datasets of simulated reference excitations were then obtained: a low (first optimisation) and a high (second optimisation) co-contraction datasets (**Fig. 2**). Similarly, 200 optimisations with random initial guesses were evaluated to determine the viable control space (shaded area in **Fig. 2**) and highlight the musculoskeletal model redundancy.

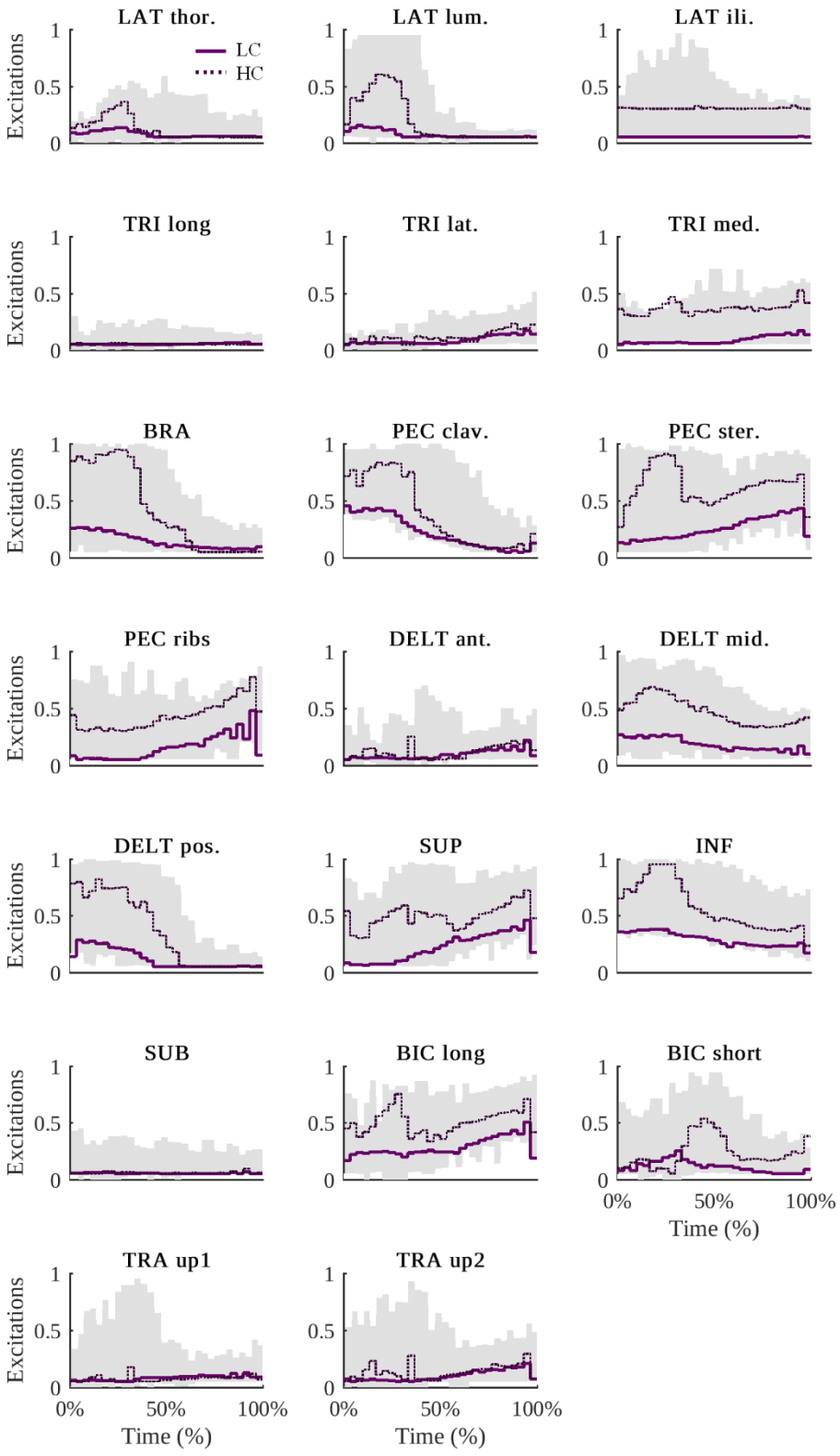

Fig. 2 Piecewise constant representation of the muscles excitations of the simulated noise-free reference movement with low (LC, light purple solid line) and high (HC, dark purple dashed line) co-contraction. The greyed areas represent the 200 different excitations solutions surface

Marker trajectories were calculated from the noise-free reference joint kinematics. Finally, zero-mean Gaussian noises were created to mimic the errors usually associated with experimental marker trajectories and EMG measurements. In line with the STA reported at the clavicle, scapula, and humerus by Blache et al. (2016) [31], the standard deviations on marker trajectories were 0.3 cm to 1.0 cm of the mean marker trajectories (0.3 cm for thorax and hand; 0.4 cm for clavicle; 0.5 cm for scapula; 0.8 cm for radius and ulna; and 1.0 cm for humerus). The standard deviation on muscle excitations was 15% of the mean excitations. This level of noise was chosen so that, when the noisy excitations were injected into the equations of dynamics (Eq. [1a-b, 4]), the joint angles ($\mathbf{q}$) reached their physiological boundaries in 0.13 ± 0.03 second.

For each dataset (*i.e.* with low and high co-contraction), the two noises (on marker trajectories and muscle excitations) were generated 30 times – further referred as to 30 *trials*. They were then added to the noise-free reference excitations and marker trajectories to introduce variability into the results.

2.3 Three optimisations comparison

Three different algorithms for estimating muscle forces were compared: two dynamic and one static optimisations. For each noisy trial, the generalised kinematics ($\mathbf{q}, \dot{\mathbf{q}}, \ddot{\mathbf{q}}$) of the musculoskeletal system was calculated first, using an extended Kalman filter [40]. Then, the calculated joint positions ($\mathbf{q}$) and velocities ($\dot{\mathbf{q}}$) were defined as initial guesses for the two dynamic optimisations; the joint positions, velocities and accelerations ($\ddot{\mathbf{q}}$) were directly used to estimate the joint torques required in static optimisation.

Both dynamic optimisations were solved using a direct multiple shooting algorithm with MUSCOD-II. Control variables were the muscle excitations ($\mathbf{e}$) and state variables were the joint angles, velocities ($\mathbf{q}, \dot{\mathbf{q}}$) and muscle activations ($\mathbf{a}$). Controls and states variables were jointly optimised with respect to each optimisation objective-function and the equation of dynamics (Eq. [4]).

2.3.1 EMG-marker tracking optimisation

In the EMG-marker tracking forward dynamics-based optimisation, the differences between the *noisy reference* and estimated marker trajectories (**M**) and excitations (**e**) were minimised using the following least-squares formulation:

$$\min_{\mathbf{e}} \sum_{i=1}^{31} W_e \|\mathbf{e_{NOISE}} - \mathbf{e}\|^2 + W_{M_{\mathrm{EMTO}}} \|\mathbf{M_{NOISE}} - \mathbf{M}(\mathbf{e})\|^2 \quad (5a)$$

subject to: Eq. [4] (5b)

$$0 \leq \mathbf{a} \leq 1 \quad (5c)$$

$$0 \leq \mathbf{e} \leq 1 \quad (5d)$$

where the NOISE-index refers to the noisy reference data; $W_{M_{\mathrm{EMTO}}}$ and W_e are the weightings on marker trajectories and excitations, respectively. The noisy reference excitations were given as initial guesses for the control variables. The initial activations were calculated from the noisy reference excitations, by solving the activation dynamics ODE (Eq. [1a-b]).

2.3.2 Marker tracking optimisation

The marker tracking forward dynamics-based optimisation consisted in finding the least-squared muscle excitations that tracked the marker trajectories, using the following objective-function:

$$\min_{\mathbf{e}} W_c \int_0^1 \mathbf{e}(t)^{\mathbf{T}} \mathbf{e}(t)\, dt + \sum_{i=1}^{31} W_{M_{\mathrm{MTO}}} \|\mathbf{M_{NOISE}} - \mathbf{M}(\mathbf{e})\|^2 \quad (6a)$$

subject to: Eq. [4] (6b)

$$0 \leq \mathbf{a} \leq 1 \quad (6c)$$

$$0 \leq \mathbf{e} \leq 1 \quad (6c)$$

where $W_c = 10^{-3}$ is the weighting on least-squared excitations and $W_{M_{\mathrm{MTO}}}$ is the weighting on marker trajectories. As the movement lasted one second, the squared

excitations $\left(\mathbf{e}(t)^{\mathbf{T}}\mathbf{e}(t)\right)$ in Eq. [6a] were integrated between 0 and 1 second. Initial muscle activations and excitations were both set at 0.08 for all muscles, all along the movement.

For both EMG-marker tracking and marker tracking dynamic optimisations, the weightings were manually adjusted, until the tracking residuals of the marker trajectories had the same order of magnitude as those obtained with the Kalman filter. They were set at: $W_e = \frac{1}{20}$, 20 corresponding to the number of lines of action, $W_{M_{\mathrm{EMTO}}} = 0.15$, $W_{M_{\mathrm{MTO}}} = 0.3$ and $W_c = 5.10^{-5}$.

2.3.3 Static optimisation

For static optimisation, joint torques were, first, calculated by inverse dynamics, using the joint kinematics resulting from the extended Kalman filter:

$$\boldsymbol{\tau}_{\mathbf{ID}}(\mathbf{q}, \dot{\mathbf{q}}, \ddot{\mathbf{q}}) = \boldsymbol{\mathcal{M}}(\mathbf{q})\ddot{\mathbf{q}} + \mathbf{N}(\mathbf{q}, \dot{\mathbf{q}})\dot{\mathbf{q}} + \mathbf{G}(\mathbf{q}) \quad (7)$$

Muscle activations **a** were then optimised at each time *t*, according to a least-squares criterion, so that the muscle joint moments ($\boldsymbol{\tau}_{\mathbf{mus}}$, see Eq. [3]) matched the joint torques given by inverse dynamics ($\boldsymbol{\tau}_{\mathbf{ID}}$):

$$\mathcal{C}_{\mathrm{SO}} = \min_{\mathbf{a}} \frac{1}{2}\,\mathbf{a}^{\mathbf{T}}\mathbf{a} \quad (8a)$$

$$\text{subject to } \boldsymbol{\tau}_{\mathbf{mus}}(\mathbf{q}, \dot{\mathbf{q}}, \mathbf{a}) = \boldsymbol{\tau}_{\mathbf{ID}}(\mathbf{q}, \dot{\mathbf{q}}, \ddot{\mathbf{q}}) \quad (8b)$$

The static optimisation problem was solved using residual actuators [41] in MATLAB (Mathworks, Nantucket, MA), *i.e.* by treating the constraints as penalties in the objective-function of a nonlinear least-squares problem. This way, 1 N.m was equivalent to 100% of the activation of one muscle.

2.4 Analysis

The marker tracking residuals were reported to assess the efficiency of each optimisation to track the given noisy reference marker trajectories ($\mathbf{M_{NOISE}}$). For static optimisation, the residual actuators (*i.e.* $\boldsymbol{\tau}_{\mathbf{mus}} - \boldsymbol{\tau}_{\mathbf{ID}}$) were also reported as an indicator of the algorithm

efficiency to manage the noise. The root mean square error (RMSe) and the bias (average error) were calculated between the noise-free reference and the estimated joint angles, muscle forces and activations. The time-integral of the squared activations was also reported to attest the marker tracking objective-function efficacy. A one-way ANOVA from the statistical parametric mapping (SPM) package [42] was used to test the *Optimisation method* effect (EMG-marker tracking *vs.* marker tracking *vs.* static optimisation) on the time-histories biases between the reference and estimated joint angles and muscle forces. The significance level was set at $p < 0.05$. When significant differences were found, Tukey post-hoc comparisons were performed. Only significant differences over a period longer than 0.2 second were reported.

3. Results

Only the results for the high co-contraction dataset are presented in this section. The results referring to the low co-contraction dataset are available in **Appendix C**.

3.1 Marker and kinematics tracking

The EMG-marker tracking and marker tracking optimisations using MUSCOD-II converged in 68.2 ± 11.9 and 56.5 ± 27.4 minutes (mean ± standard deviation of n = 30 trials), respectively, for an average of 6 million calls of the forward-dynamic function (Intel® Core™ i5-3570 CPU @3.4 GHz). Comparatively, static optimisation on MATLAB converged in 2.2 ± 1.0 minutes. For static optimisation, the average residual actuator was - 0.23 ± 0.58 N.m, which is good.

The tracking residuals of the marker trajectories had the same order of magnitude for the three optimisations (EMG-marker tracking: 0.31 ±0 .32 cm; marker tracking: 0.43 ± 0.30 cm; static optimisation: 0.17 ± 0.06 cm). Markers placed on the distal segments of the kinematic chain had larger errors than those placed on the proximal segments (see **Appendix B**). On average, the bias and RMSe values of the estimated joint angles qualitatively showed small differences for the three optimisations (**Table 2**). However, for the elbow flexion, the SPM ANOVA revealed a significant effect of the *Optimisation method* on the biases between the reference and the estimated joint angle (**Fig. 3**). Post-hoc comparisons then indicated that the marker tracking biases were significantly different from the EMG-marker tracking ones and from static optimisation ones. Marker tracking and static optimisations biases were never significantly different.

Please insert Table 2 here

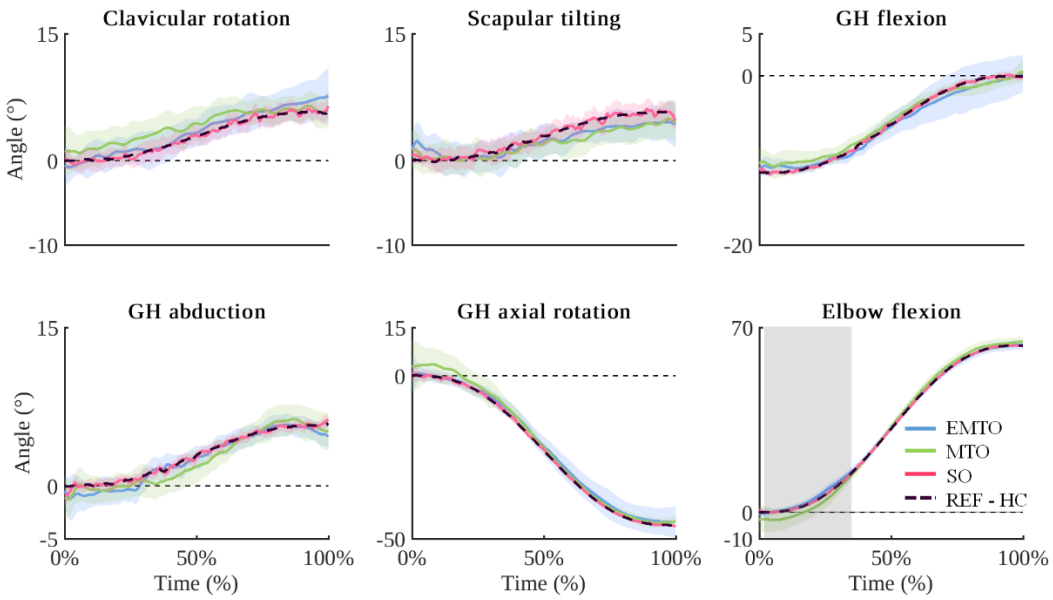

Fig. 3 Reference (REF-HC) and mean ± standard deviation of the estimated joint angles obtained with the high co-contraction dataset. Grey-shaded zones represent the SPM ANOVA results, *i.e.* the time intervals where there is a significant *Optimisation method* effect

3.2 Muscle activations and forces

The time integral of the squared activations was 15.0 for the reference, 16.1 ± 14.0 for the EMG-marker tracking optimisation, 1.2 ± 1.1 for the marker tracking optimisation and 11.7 ± 8.5 for static optimisation. Concerning the muscle forces, the EMG-marker tracking RMSe averaged across all the lines of action was 20.39 ± 13.24 N, with a bias of 3.25 ± 4.78 N meaning a small overestimation (**Table 3**). RMSe for marker tracking and static optimisations were about seven times larger than for EMG-marker tracking (124.22 ± 118.22 N and 148.15 ± 94.01 N, respectively), with average negative biases, *i.e.* muscle forces were underestimated. Static optimisation showed the largest inter-trial variability in muscle forces and activations estimations (see biases standard deviations in **Tables 3** and **4**).

Please insert Table 3 here

Please insert Table 4 here

The SPM ANOVA revealed a significant effect of the *Optimisation method* on the biases between the reference and estimated muscle forces: on more than 95% of the movement for eight muscles (LAT ili., TRI med., PEC ster., PEC ribs, DELT mid., SUP, INF and BIC long); on at least 50% of the movement for five muscles (LAT lum., TRI lat., BRA., PEC clav. and DELT pos.); on less than 35% of the movement for two muscles (LAT thor. and BIC short). No significant difference lasting more than 0.2 s was observed for the other muscles (**Fig. 4**). For the fifteen abovementioned muscles, post-hoc comparisons indicated that the biases between the reference and estimated muscle forces were significantly smaller with the EMG-marker tracking optimisation than with the marker tracking optimisation. The EMG-marker tracking and static optimisations biases were significantly different too. For three muscles only (LAT thor., SUP and INF), a significant difference was also revealed between the marker tracking and static optimisations biases.

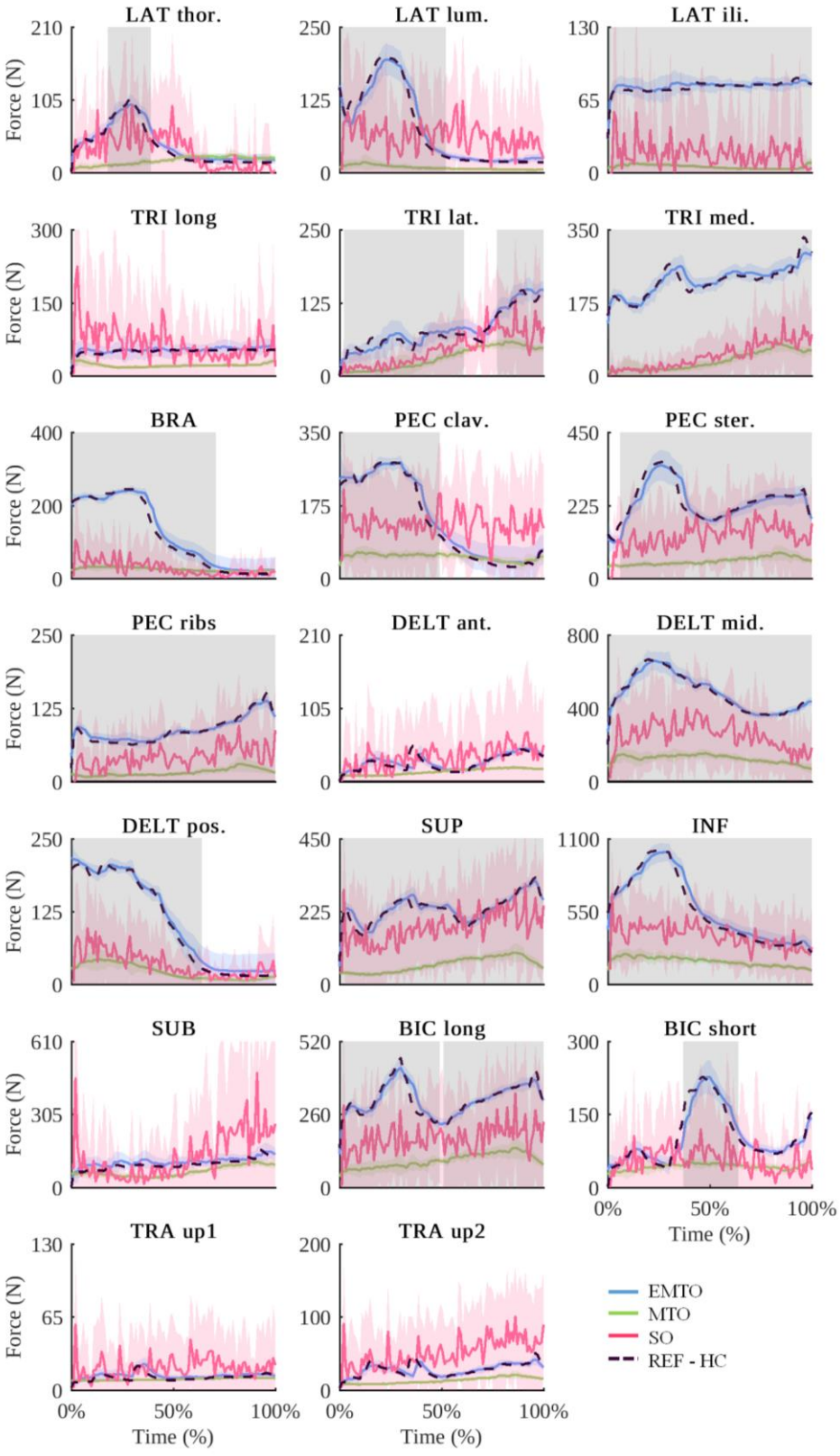

Fig. 4 Reference (REF-HC) and mean ± standard deviation of the estimated muscle forces obtained with the high co-contraction dataset. Grey-shaded zones represent the SPM ANOVA results, *i.e.* the time intervals where there is a significant *Optimisation method* effect

4. Discussion

The main objective of this study was to assess the efficiency of an innovative EMG-marker tracking optimisation in its ability to estimate muscle forces. The forward dynamic problem was solved using a direct multiple shooting algorithm in MUSCOD-II that was never used for a musculoskeletal model to date, to the best of our knowledge. Based on simulated data, our main finding was that tracking both muscle excitations and marker trajectories in a forward dynamics-based optimisation led to accurate muscle force estimates, in a few minutes only. By comparison to the least-activation/excitation static and dynamic optimisations, the error on muscle forces was reduced by six to seven times. Finally, the EMG-marker tracking optimisation presented a small inter-trial variability, highlighting its robustness to noise.

4.1 Optimisations comparison

The three optimisations tracked well the markers and qualitatively resulted in similar marker kinematics. In this respect, the EMG-marker tracking optimisation proved its ability to reproduce the reference movement, while noisy excitations would tend to make the solution diverge exponentially. Hence, although it is commonly admitted that accurately tracking the kinematics using a forward dynamics-based optimisation is challenging [5, 25], our innovative approach succeeded to give as good results as static optimisation (see biases in **Table 2**), even if two different sources of information were combined. Since estimated kinematics are qualitatively comparable between the three optimisations, we may discuss the muscle forces differences.

As expected, for 15 out of 20 lines of action, the EMG-marker tracking optimisation produced significantly smaller force biases than did the marker tracking and static optimisations. Therefore, using muscle excitations and marker trajectories as input gave good forces estimations, compared to existing musculoskeletal models that tracked only joint kinematics, for instance [25, 39]. Interestingly, for the TRI lat. and TRI med. acting as antagonists during the studied movement, the estimated muscle forces were smaller with

the two least-activation/excitation optimisations than with the EMG-marker tracking optimisation. In other words, in the high co-contraction condition, the forces estimations of the antagonistic muscles were more accurate with the EMG-marker tracking approach than with static optimisation or marker tracking alone. This result emphasizes that using a least-activation/excitation criterion may not be the most relevant method to physiologically estimate all muscle forces [12, 43]. The EMG-marker tracking algorithm would thus be recommended especially when evaluating movements with high co-contraction.

Compared to the reference, both static and marker-tracking optimisations based on least-activation/excitation criteria underestimated muscle forces. The latter were close to each other with a 23.9 N difference between their respective mean RMSe (**Table 3**). This observation is in accordance with Anderson and Pandy (2001) [5], who showed that static and dynamic least-activation/excitation-based optimisations provided equivalent results for gait. Conversely, Morrow et al. (2014) [15] observed different estimated muscle forces between static and dynamic optimisations during wheelchair propulsion. They stressed that these differences may come from the need of dynamic co-contraction and the influence of the activation dynamics in such propulsion task, compared with gait. However, musculoskeletal models (including muscle-tendon equilibrium or not), movements (simulated or experimental), and algorithms (including contact forces or not) were different between the present and cited studies. Further research is therefore needed to determine the aspects underlying the differences between static and dynamic optimisations and to identify the most relevant methods according to the joints and/or movements of interest to estimate muscle forces.

Interestingly, the two dynamic optimisations presented a limited inter-trial variability in comparison to static optimisation, highlighting their smaller sensitivity to noise (**Table 3**). Their better performance may be explained by the muscles dynamic properties. In fact, while excitations were discretized into a piecewise constant representation in MUSCOD-II, activations remained continuous due to the multiple integrations over time (Eq. [1a-b]). This resulted in muscles forces, joint torques and accelerations smoother than those

obtained with inverse kinematics/dynamics, *i.e.* with static optimisation. The slight overestimation observed with the proposed method (+3.25 ± 4.78 N) may be explained by the use of a Gaussian noise associated to 10 and 40 ms time constants in the activation dynamics ODE (Eq. [1a-b]). Consequently, forward dynamics-based optimisations should be preferred, especially as the EMG-marker tracking optimisation gave the best agreement between the estimated and reference muscle forces, with low variability.

4.2 Algorithm novelties

In the EMG-marker tracking optimisation, both muscle excitations and marker trajectories were used in the same objective-function. To the best of our knowledge, no study has simultaneously tracked EMG and marker trajectories to estimate muscle forces yet. For instance, Raison et al. (2011) [34] and Lloyd and Besier (2003) [29] used experimental EMG and marker data but in a hybrid approach (*i.e.* inverse-forward algorithm), whose main limitation is the propagation of errors into the kinematics when tracking the joint torques.

The dynamic optimisations joint angles RMSe (< 3°) were comparable to those obtained in the literature, ~5° [17]. Several aspects of the proposed study may explain this accurate tracking: the performance of MUSCOD-II to solve forward-dynamic problems [23]; weightings on the different objective-function terms; and the tracking of markers instead of joint angles or torques [25, 44]. This choice avoided to weight each joint according to its range of motion [15] and, above all, to make errors propagate through the model kinematic chain.

The convergence time of the two forward dynamic-based optimisations (~60 min) was longer than that of the computed muscle control [17], but faster than previous dynamic optimisations [16]. In fact, in our dynamic optimisations resolution with MUSCOD-II, the convergence time greatly depended on the solution accuracy (quantified by the Karush-Kuhn-Tucker tolerance value), pre-specified to the software as a termination criterion (here set at 10^{-6}) [23]. The fact remains that the direct multiple shooting algorithm was an

efficient method to solve our musculoskeletal problem. Indeed, the kinematics fast divergence when adding noise to the excitations (joints limits attained after 0.13 ± 0.03 second) would have resulted in infeasible convergence using algorithms traditionally implemented to solve musculoskeletal problems.

Future work comparing our EMG-marker tracking approach to other approaches estimating muscle forces in the literature – such as the CEINMS toolbox [45], in which both muscle excitations and joint moments are tracked – could be of interest to identify the optimal objective-function.

4.3 From simulation to real data

In this paper, we mainly focused on developing and evaluating a new tracking-assisted optimisation method. We thus chose to keep simple the model and data, as well as the studied movement. Accordingly, simulated data were preferred to experimental measurements to quantify the error of each optimisation method, as it allowed us to have an essential set of *reference* values. Muscle excitations were therefore generated with an arbitrary enforced co-contraction criterion. Besides, Gaussian noises were added to the marker trajectories and excitations to simulate the artefacts existing on real data. At this stage, our results are not physiological. In future studies, the EMG-marker tracking algorithm should be run using experimental EMG and marker trajectories. As experimental EMG is inherently noisy [27], it should be carefully treated and amplitude-normalized – in line with previous research [46, 47] –, while using the EMG-marker tracking approach. Indeed, the EMG signal quality is known to affect the muscle forces estimations, regardless of the method used to estimate them, as stressed by [45]. Furthermore, since deep muscles are difficult to access with surface EMG, the robustness of our EMG-marker tracking algorithm using partial EMG data should also be assessed in a near future.

In the same vein, we chose to work with a simple generic musculoskeletal model. The later was developed from two separate studies to determine all the muscle parameters [36, 37], as no complete upper-limb muscle database could have been found in the literature.

Consequently, the model could be refined using additional lines of action (e.g., Delp et al. (2007) [41]), series elasticity and the muscle-tendon force equilibrium [48]. The muscle-tendon parameters could also be personalized. In the real case, these parameters are either obtained from the literature (mean values measured from cadavers) [49] or from generic models using regression equations [50] or optimisation [51]. The fact is that real muscle-tendon parameters have errors on them that might affect the muscle forces estimations. To address this problem, muscle-tendon parameters are usually weighted while calibrating the model and tuned to the subject using static optimisation [29, 51, 52]. In future developments of our work, the model could be calibrated from experimental data using the EMG-marker tracking algorithm to adjust the muscle-tendon parameters; muscle forces would be then estimated, still with the same approach. The direct multiple shooting algorithm will allow such identification of the musculotendinous parameters, as, for example, the maximal isometric force.

5. Conclusion

In conclusion, the innovative forward dynamics-based optimisation proposed in our study, solved with a direct multiple shooting algorithm, successfully estimated the upper-limb muscle forces, with smaller errors than static and dynamic least-activation/excitation optimisations. Indeed, our innovative approach with both simulated EMG and marker trajectories tracking improved muscle forces biofidelity and accuracy, while commonly used optimisations failed to reproduce muscle co-contraction.

Acknowledgments Funding for this project was provided by the NSERC Discovery grant (RGPIN-2014-03912). The first and second authors received a MÉDITIS and GRSTB scholarship, respectively. Also, we thank the Optimization in Robotics and Biomechanics research group of the IWR at the University of Heidelberg for giving us the possibility to work with MUSCOD-II.

Appendix

Appendix A

A.1 The MUSCOD-II software

MUSCOD-II [23] solves optimal control problems based on the direct multiple shooting algorithm [22, 53]. The latter consists in dividing the integration interval in N shorter sub-intervals, which facilitates and speeds up the convergence of the solution [24]. Additional matching constraints guarantee the continuity of the overall solution over the whole time interval. Inequality constraints are also applied, as, for instance, the ranges of joint angles ($\mathbf{q}$), velocities ($\dot{\mathbf{q}}$), muscle activations ($\mathbf{a}$) and excitations ($\mathbf{e}$):

$$\mathbf{q_{min}} \leq \mathbf{q} \leq \mathbf{q_{max}} \quad (9a)$$

$$\dot{\mathbf{q}}_{\mathbf{min}} \leq \dot{\mathbf{q}} \leq \dot{\mathbf{q}}_{\mathbf{max}} \quad (9b)$$

$$0 \leq \mathbf{a} \leq 1 \quad (9c)$$

$$0 \leq \mathbf{e} \leq 1 \quad (9d)$$

In the present study, MUSCOD-II was used with the $4^{th}/5^{th}$ ODE/DAE Runge-Kutta-Fehlberg solver module, which has a good accuracy level for a given time step [54].

A.2 Reference muscle excitations generation

From an anatomical position, the simulated noise-free reference movement mainly consisted of an elbow flexion, hand palm facing upward. The desired joint angles and velocities were defined using the Yeadon *quintic* spline functions [55]. MUSCOD-II [23] was then used to obtain the reference muscle excitations that produced the desired joint kinematics. Control variables were the muscle excitations ($\mathbf{e}$) and state variables were the joint angles, velocities ($\mathbf{q}$, $\dot{\mathbf{q}}$) and muscle activations ($\mathbf{a}$). Controls and states variables were jointly optimised with respect to each optimisation objective-function and the equation of dynamics (Eq. [4]). No objective-function was given while generating the optimal noise-free reference excitations with MUSCOD-II. The movement duration was fixed at 1 second. All aforementioned inequality constraints (Eq. [9a-d]) were specified. Specifically,

joint angles were forced to respect the desired kinematic values, given as initial solution, at each node of the problem.

Appendix B

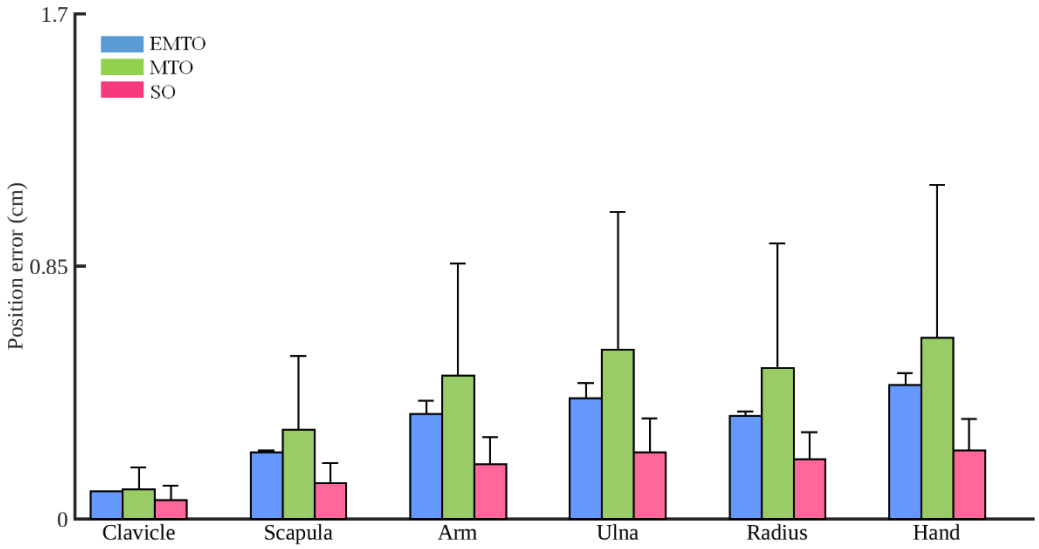

Fig. 5 Tracking residual of the markers for the three optimisations, averaged across all the markers, across the duration of the movement with high co-contraction and across the 30 trials. *Note.* The EMTO, MTO and SO acronyms stand for the EMG-marker tracking, marker tracking and static optimisations, respectively

Appendix C: Results for the low co-contraction movement

C.1 Marker and kinematics tracking

The EMG-marker tracking and marker tracking optimisations using MUSCOD-II converged in 25.5 ± 5.3 and 73.9 ± 49.0 minutes (mean ± standard deviation of $n = 30$ trials), respectively, for an average of 3.6 million calls of the forward-dynamic function (Intel® Core™ i5-3570 CPU @3.4 GHz). Comparatively, static optimisation on MATLAB converged in 2.5 ± 1.0 minutes. The average residual actuator in static optimisation was - 0.17 ± 0.49 N.m, which is good.

Similarly to the high co-contraction movement, the tracking residuals of the marker trajectories had the same order of magnitude for the three optimisations (EMG-marker tracking: 0.23 ± 0.10 cm; marker tracking: 0.24 ± 0.11 cm; static optimisation: 0.17 ± 0.06 cm). Errors were larger for markers placed on the distal segments of the kinematic chain than for those placed on the proximal segments (**Fig. 6**).

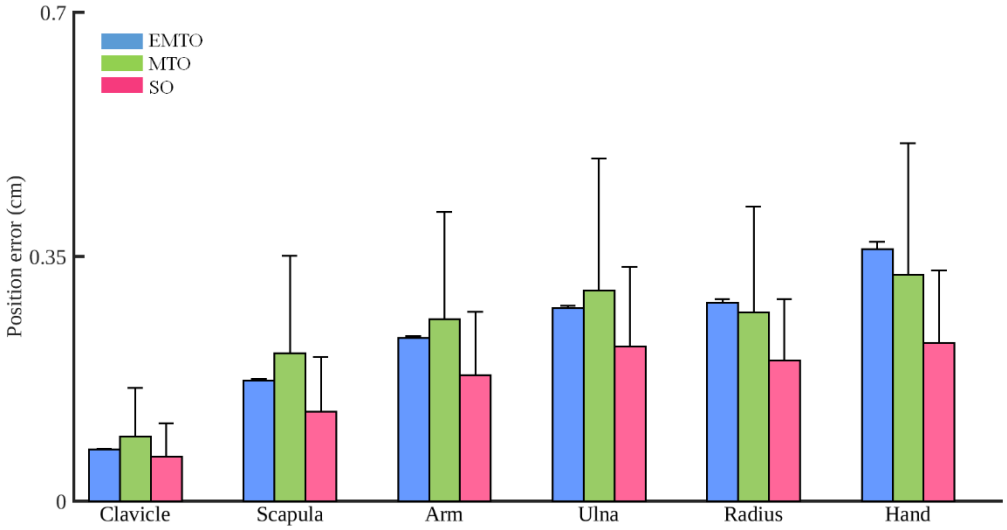

Fig. 6 Tracking residual of the markers for the three optimisations, averaged across all the markers, across the length of the movement with low co-contraction and across the 30 trials. *Note.* The EMTO, MTO and SO acronyms stand for the EMG-marker tracking, marker tracking and static optimisations, respectively

The bias and RMSe values of the estimated joint angles were similar between the three optimisations (**Table 5**). The SPM ANOVA thus revealed no significant effect of the *Optimisation method* on the biases between the reference and the estimated joint angle lasting more than 0.2 s, for any DOF (**Fig. 7**).

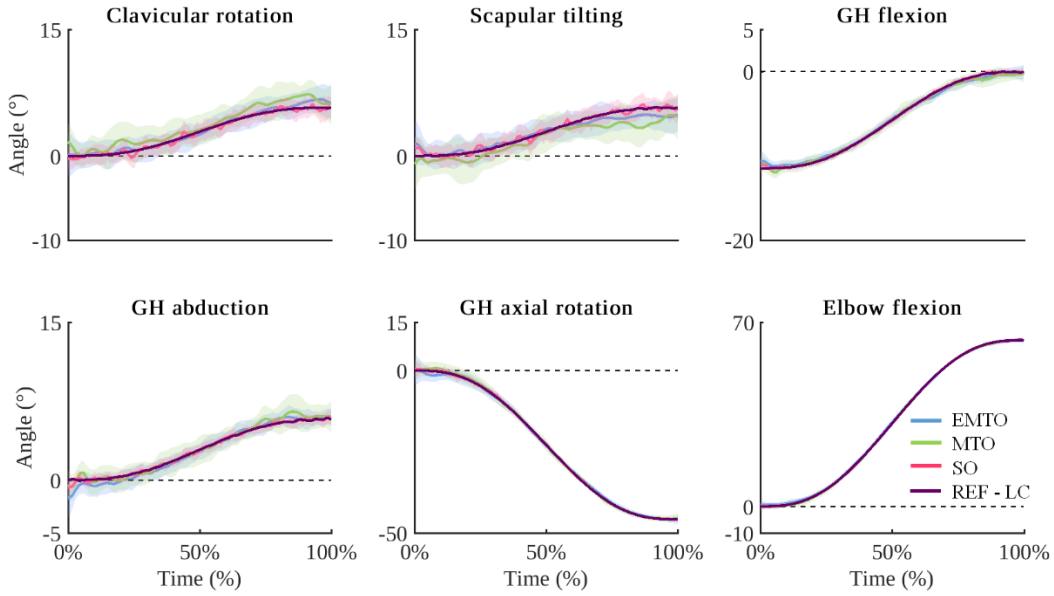

Fig. 7 Reference (REF-LC) and mean ± standard deviation of the estimated joint angles obtained with the low co-contraction dataset. Grey-shaded zones represent the SPM ANOVA results, *i.e.* the time intervals where there is a significant *Optimisation method* effect

Please insert Table 5 here

C.2 Muscle activations and forces

The time integral of the squared activations averaged across all the lines of action was 2.9 for the reference, 3.2 ± 3.2 for the EMG-marker tracking optimisation, 1.2 ± 1.1 for the marker tracking optimisation and 11.4 ± 8.2 for static optimisation. Concerning the muscle forces, the EMG-marker tracking RMSe averaged across all the lines of action was 7.61 ± 4.83 N with a bias of 2.2 ± 3.6 N, meaning a small overestimation (**Table 6**). RMSe for marker tracking (34.71 ± 29.44 N) and static (115.51 ± 75.74 N) optimisations presented a five- and sixteen-fold increase, respectively, with systematically negative biases for marker tracking optimisation (*i.e.* forces were underestimated for all muscles)

and a positive average bias for static optimisation (**Table 6**). Muscle forces and activations in static optimisation showed the largest inter-trial variability (see biases standard deviations in **Tables 6** and **7**).

Please insert Table 6 here

Please insert Table 7 here

For INF, the SPM ANOVA revealed a significant effect of the *Optimisation method* on the biases between the reference and estimated muscle forces on more than 50% the movement (**Fig. 8**). For TRI lat., TRI med. and PEC clav., the significant *Optimisation method* effect was observed on less than 50% of the movement. No significant difference lasting more than 0.2 s was observed for the other muscles. For TRI lat. and TRI med., post-hoc only assessed that the EMG-marker tracking biases were significantly different from the marker tracking ones and from static optimisation ones (*i.e.* marker tracking and static optimisations biases were never significantly different, for these two muscles). For INF, post-hoc comparisons only indicated that the marker tracking biases were significantly different from the EMG-marker tracking ones and from static optimisation ones. For PEC clav., post-hoc comparisons showed that the EMG-marker tracking biases were significantly different from the marker tracking ones and from static optimisation ones; and that the marker tracking and static optimisations biases were significantly different too.

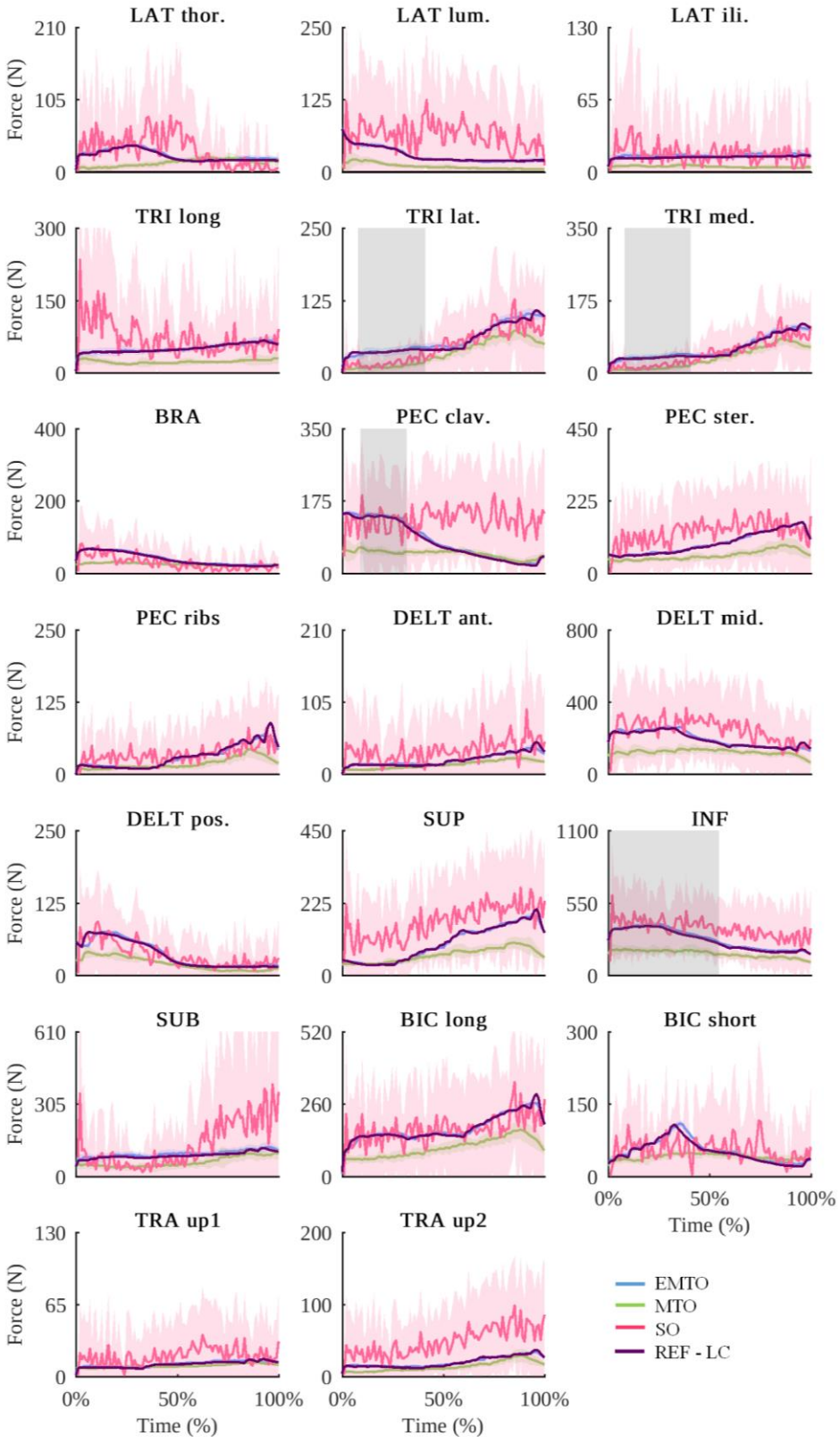

Fig. 8 Reference (REF-LC) and mean ± standard deviation of the estimated muscle forces obtained with the low co-contraction dataset. Grey-shaded zones represent the SPM

ANOVA results, *i.e.* the time intervals where there is a significant *Optimisation method* effect

References

1. Eberhard, P., T. Spagele, and A. Gollhofer: Investigations for the Dynamical Analysis of Human Motion, *Multibody System Dynamic* **3**, 1-20, (1999).
2. Valero-Cuevas, F.J., B.A. Cohn, H.F. Yngvason, and E.L. Lawrence: Exploring the high-dimensional structure of muscle redundancy via subject-specific and generic musculoskeletal models, *Journal of Biomechanics* **48**(11), 2887-96, (2015).
3. Erdemir, A., S. McLean, W. Herzog, and A.J. van den Bogert: Model-based estimation of muscle forces exerted during movements, *Clinical Biomechanics* **22**(2), 131-54, (2007).
4. Crowninshield, R.D. and R.A. Brand: A physiologically based criterion of muscle force prediction in locomotion, *Journal of Biomechanics* **14**(11), 793-801, (1981).
5. Anderson, F.C. and M.G. Pandy: Static and dynamic optimization solutions for gait are practically equivalent, *Journal of Biomechanics* **34**(2), 153-61, (2001).
6. DeMers, M.S., S. Pal, and S.L. Delp: Changes in tibiofemoral forces due to variations in muscle activity during walking, *Journal of Orthopaedic Research* **32**(6), 769-76, (2014).
7. Heintz, S. and E.M. Gutierrez-Farewik: Static optimization of muscle forces during gait in comparison to EMG-to-force processing approach, *Gait Posture* **26**, 279-88, (2007).
8. Kim, H.J., J.W. Fernandez, M. Akbarshahi, J.P. Walter, B.J. Fregly, and M.G. Pandy: Evaluation of predicted knee-joint muscle forces during gait using an instrumented knee implant, *Journal of Orthopaedic Research* **27**(10), 1326-31, (2009).
9. Darainy, M. and D.J. Ostry: Muscle cocontraction following dynamics learning, *Experimental Brain Research* **190**(2), 153-63, (2008).
10. Blache, Y., F. Dal Maso, L. Desmoulins, A. Plamondon, and M. Begon: Superficial shoulder muscle co-activations during lifting tasks: Influence of lifting height, weight and phase, *Journal of Electromyography and Kinesiology* **25**(2), 355-62, (2015).
11. Veeger, H.E.J. and F.C.T. Van Der Helm: Shoulder function: the perfect compromise between mobility and stability, *Journal of Biomechanics* **40**(10), 2119-29, (2007).
12. Cholewicki, J., S.M. McGill, and R.W. Norman: Comparison of muscle forces and joint load from an optimization and EMG assisted lumbar spine model: towards development of a hybrid approach, *Journal of Biomechanics* **28**(3), 321-31, (1995).
13. Ackermann, M. and W. Schiehlen, *Physiological Methods to Solve the Force-Sharing Problem in Biomechanics*, in *Multibody Dynamics - Computational Methods and Applications*, C.L. Bottasso, Editor. 2009, Springer.

14. Pandy, M.G.: Computer Modelling and Simulation of Human Movement, *Annual Review of Biomedical Engineering* **3**, 245-73, (2001).
15. Morrow, M.M., J.W. Rankin, R.R. Neptune, and K.R. Kaufman: A comparison of static and dynamic optimization muscle force predictions during wheelchair propulsion, *Journal of Biomechanics* **47**(14), 3459-65, (2014).
16. Neptune, R.R.: Optimization algorithm performance in determining optimal controls in human movement analyses, *Journal of Biomechanical Engineering* **121**(2), 249-52, (1999).
17. Thelen, D.G. and F.C. Anderson: Using computed muscle control to generate forward dynamic simulations of human walking from experimental data, *Journal of Biomechanics* **39**, 1107-15, (2006).
18. Ackermann, M. and A.J. van den Bogert: Optimality principles for model-based prediction of human gait, **43**, 1055–60, (2010).
19. De Groote, F., A.L. Kinney, A.V. Rao, and B.J. Fregly: Evaluation of direct collocation optimal control problem formulations for solving the muscle redundancy problem, *Annals of Biomedical Engineering* **44**(10), 2922-36, (2016).
20. Meyer, A.J., I. Eskinazi, J.N. Jackson, A.V. Rao, C. Patten, and B.J. Fregly: Muscle Synergies Facilitate Computational Prediction of Subject-specific Walking Motions, *Frontiers in bioengineering and biotechnology* **4**, 77, (2016).
21. Lin, Y.C. and M.G. Pandy: Three-dimensional data-tracking dynamic optimization simulations of human locomotion generated by direct collocation, *Journal of Biomechanics* **[in press]**, (2017).
22. Mombaur, K., J.-P. Laumond, and E. Yoshida: An Optimal Control-Based Formulation to Determine Natural Locomotor Paths for Humanoid Robots, *Advanced Robotics* **24**, 515-35, (2010).
23. Leineweber, D.B., I. Bauer, H.G. Bock, and J.P. Schloder: An efficient multiple shooting based reduced SQP strategy for large-scale dynamic process optimization. Part 1: theoretical aspects, *Computers & Chemical Engineering* **27**(2), 157-66, (2003).
24. Spagele, T., Kistner, A., Gollhofer, A.: A multi-phase optimal control technique for the simulation of a human vertical jump, *Journal of Biomechanics* **32**, 87-91, (1999).
25. Neptune, R.R., S.A. Kautz, and F.E. Zajac: Contributions of the individual ankle plantar flexors to support, forward progression and swing initiation during walking, *Journal of Biomechanics* **34**(11), 1387-98, (2001).
26. Neptune, R.R., I.C. Wright, and A.J. van den Bogert: A method for numerical simulation of single limb ground contact events: application to heel-toe running, *Computer Methods in Biomechanics and Biomedical Engineering* **3**, 321-34, (2000).

27. Chowdhury, R.H., M.B.I. Reaz, M.A.B.M. Ali, A.A.A. Bakar, K. Chellappan, and T.G. Chang: Surface Electromyography Signal Processing and Classification Techniques, *Sensors* **13**, 12431-66, (2013).
28. Amarantini, D. and L. Martin: A method to combine numerical optimization and EMG data for the estimation of joint moments under dynamic conditions, *Journal of Biomechanics* **37**(9), 1393-404, (2004).
29. Lloyd, D.G. and T.F. Besier: An EMG-driven musculoskeletal model to estimate muscle forces and knee joint moments in vivo, *Journal of Biomechanics* **36**(6), 765-76, (2003).
30. Matsui, K., K. Shimada, and P.D. Andrew: Deviation of skin marker from bone target during movement of the scapula, *Journal of Orthopaedic Science* **11**(2), 180-4, (2006).
31. Blache, Y., R. Dumas, A. Lundberg, and M. Begon: Main component of soft tissue artifact of the upper-limbs with respect to different functional, daily life and sports movements, *Journal of Biomechanics* **[in press]**, (2016).
32. Challis, J.H. and M.T. Pain: Soft tissue motion influences skeletal loads during impacts, *Exercise and Sport Sciences Reviews* **36**(2), 71-5, (2008).
33. Günther, M., V.A. Sholukha, D. Kessler, V. Wank, and R. Blickhan: Dealing with skin motion and wobbling masses in inverse dynamics, *Journal of Mechanics in Medicine and Biology* **3**(03n04), 309-35, (2003).
34. Raison, M., C. Detrembleur, P. Fisette, and J.-C. Samin, *Assessment of Antagonistic Muscle Forces During Forearm Flexion/Extension*, in *Multibody Dynamics - Computational Methods and Applications*, K. Arczewski, et al., Editors. 2011, Springer.
35. Felis, M. *Rigid Body Dynamic Library (RBDL)*. 2011; Available from: http://rbdl.bitbucket.org/.
36. Holzbaur, K.R., W.M. Murray, and S.L. Delp: A model of the upper extremity for simulating musculoskeletal surgery and analyzing neuromuscular control, *Annals of Biomedical Engineering* **33**(6), 829-40, (2005).
37. van der Helm, F.C.: Analysis of the kinematic and dynamic behavior of the shoulder mechanism, *Journal of Biomechanics* **27**(5), 527-50, (1994).
38. Zajac, F.E.: Muscle and tendon: properties, models, scaling, and application to biomechanics and motor control, *Critical Reviews in Biomedical Engineering* **17**(4), 359-411, (1989).
39. Thelen, D.G., F.C. Anderson, and S.L. Delp: Generating dynamic simulations of movement using computed muscle control, *Journal of Biomechanics* **36**, 321-8, (2003).

40. Fohanno, V., M. Begon, P. Lacouture, and F. Colloud: Estimating joint kinematics of a whole body chain model with closed-loop constraints, *Multibody System Dynamics* **31**(4), 433-49, (2014).
41. Delp, S.L., F.C. Anderson, A.S. Arnold, P. Loan, A. Habib, C.T. John, E. Guendelman, and D.G. Thelen: OpenSim: Open-Source Software to Create and Analyze Dynamic Simulations of Movement, *IEEE Transactions on Biomedical Engineering* **54**(11), 1940-9, (2007).
42. Friston, K.J., J.T. Ashburner, S.J. Kiebel, T.E. Nichols, and W.D. Penny, *Statistical Parametric Mapping: The Analysis of Functional Brain Images*. 2011: Academic press.
43. Forster, E., U. Simon, P. Augat, and L. Claes: Extension of a state-of-the-art optimizaation criterion to predict co-contraction, *Journal of Biomechanics* **37**, 557-81, (2004).
44. Shourijeh, M.S., K.B. Smale, B.M. Potvin, and D.L. Benoit: A forward-muscular inverse-skeletal dynamics framework for human musculoskeletal simulations, *Journal of Biomechanics* **49**(9), 1718-23, (2016).
45. Pizzolato, C., D.G. Lloyd, M. Sartori, E. Ceseracciu, T.F. Besier, B.J. Fregly, and M. Reggiani: CEINMS: A toolbox to investigate the influence of different neural control solutions on the prediction of muscle excitation and joint moments during dynamic motor tasks, *Journal of biomechanics* **48**(14), 3929-36, (2015).
46. Hermens, H.J., B. Freriks, C. Disselhorst-Klug, and G. Rau: Development of recommendations for SEMG sensors and sensor placement procedures, *Journal of electromyography and kinesiology* **10**(5), 361-74, (2000).
47. Burden, A.: How should we normalize electromyograms obtained from healthy participants? What we have learned from over 25years of research., *Journal of electromyography and kinesiology* **20**(6), 1023-35, (2010).
48. Millard, M., T. Uchida, A. Seth, and S.L. Delp: Flexing computational muscle: modeling and simulation of musculotendon dynamics, *Journal of Biomechanical Engineering* **135**(2), 021005, (2013).
49. Langenderfer, J., S. LaScalza, A. Mell, J.E. Carpenter, J.E. Kuhn, and R.E. Hughes: An EMG-driven model of the upper extremity and estimation of long head biceps force, *Computers in Biology and Medicine* **35**, 25-39, (2005).
50. Anderson, D.E., J.M. D'Agostino, A.G. Bruno, R.K. Manoharan, and M.L. Bouxsein: Regressions for estimating muscle parameters in the thoracic and lumbar trunk for use in musculoskeletal modeling, *Journal of Biomechanics* **45**(1), 66-75, (2012).
51. Menegaldo, L.L. and L.F. Oliveira: The influence of modeling hypothesis and

experimental methodologies in the accuracy of muscle force estimation using EMG-driven models., *Multibody System Dynamics* **28**(1), 21-36, (2012).

52. Buchanan, T.S., D.G. Lloyd, K. Manal, and T.F. Besier: Neuromusculoskeletal modeling: estimation of muscle forces and joint moments and movements from measurements of neural command, *Journal of Applied Biomechanics* **20**(4), 367-95, (2004).
53. Felis, M., *Modeling Emotional Aspects in Human Locomotion*, in *Combined Faculty for the Natural Sciences and Mathematics*. 2015, University of Heidelberg, Germany. p. 170.
54. Chadwick, E.K., D. Blana, A.J. van den Bogert, and R.F. Kirsch: A real-time, 3-D musculoskeletal model for dynamic simulation of arm movements, *IEEE Transactions on Biomedical Engineering* **56**(4), 941-8, (2009).
55. Yeadon, M.R.: The simulation of aerial movement - I. The determination of orientation angles from film data, *Journal of Biomechanics* **23**, 59-66, (1990).

Tables

Table 1 List of the muscles included in the model, each represented by one line of action, except for the trapezius upper fibers that are represented by two lines of action, for a total of 20 lines of actions. The muscles abbreviations and the joint(s) they cross are also mentioned

Muscles	**Abbreviations**	**Joints crossed**
Thoracic latissimus dorsi	LAT thor.	Glenohumeral
Lumbar latissimus dorsi	LAT lum.	Glenohumeral
Iliac latissimus dorsi	LAT ili.	Glenohumeral
Triceps brachii long head	TRI long	Glenohumeral and elbow
Triceps brachii lateral head	TRI lat.	Elbow
Triceps brachii medial head	TRI med.	Elbow
Brachioradialis	BRA	Elbow
Clavicular pectoralis major	PEC clav.	Glenohumeral
Sternal pectoralis major	PEC ster.	Glenohumeral
Ribs pectoralis major	PEC ribs	Glenohumeral
Anterior deltoid	DELT ant.	Glenohumeral
Middle deltoid	DELT mid.	Glenohumeral
Posterior deltoid	DELT pos.	Glenohumeral
Supraspinatus	SUP	Glenohumeral
Infraspinatus	INF	Glenohumeral
Subscapularis	SUB	Glenohumeral
Biceps brachii long head	BIC long	Glenohumeral and elbow
Biceps brachii short head	BIC short	Glenohumeral and elbow
Trapezius upper fibers (1)	TRA up1	Scapulothoracic
Trapezius upper fibers (2)	TRA up2	Scapulothoracic

Table 2 RMSe and bias in degrees between the noise-free reference and estimated DOFs of the model with high co-contraction. *Note.* GH: glenohumeral; SD: standard deviation. The EMTO, MTO and SO acronyms stand for the EMG-marker tracking, marker tracking and static optimisations, respectively. An asterisk was added next to the DOF for which a significant *Optimisation method* effect was observed on **Fig. 3**.

DOFs	**Angles (°) (mean ± sd)**					
	EMTO		**MTO**		**SO**	
	RMSe	**Bias**	**RMSe**	**Bias**	**RMSe**	**Bias**
Clavicular rotation	2.01 ± 0.70	0.57 ± 1.98	2.21 ± 0.67	1.22 ± 1.88	1.16 ± 0.09	-0.01 ± 1.15
Scapular tilting	2.08 ± 0.41	-0.56 ± 1.87	2.07 ± 0.40	-0.81 ± 1.80	1.27 ± 0.11	0.03 ± 1.25
GH flexion	1.01 ± 1.49	-0.19 ± 1.55	1.11 ± 0.46	0.29 ± 1.02	0.36 ± 0.03	0.02 ± 0.35
GH abduction	1.22 ± 0.30	-0.34 ± 1.12	1.47 ± 0.45	-0.41 ± 1.37	0.55 ± 0.06	-0.03 ± 0.52
GH axial rotation	2.18 ± 2.68	1.02 ± 3.15	2.93 ± 1.97	1.44 ± 2.62	0.90 ± 0.13	0.00 ± 0.80
Elbow flexion*	1.30 ± 0.87	0.22 ± 1.47	2.30 ± 2.01	-0.25 ± 2.41	0.48 ± 0.06	0.02 ± 0.45
MEAN(mean) ± SD(mean)	**1.63 ± 0.51**	**0.12 ± 0.60**	**2.02 ± 0.64**	**0.25 ± 0.91**	**0.79 ± 0.38**	**0.01 ± 0.02**

Table 3 RMSe and bias between the noise-free reference and estimated muscle forces with high co-contraction (n = 30 trials), for the 20 lines of action of the model. *Note.* A positive bias corresponds to an overestimation. An asterisk was added next to the muscle for which a significant *Optimisation method* effect was observed on **Fig. 4**. Post-hoc comparisons systematically reported that the bias was significantly smaller with EMTO than with MTO or SO. TRI long, TRI lat., TRI med. were the main antagonists to the movement studied.

Muscle lines of action	**Forces** (N) (**mean ± sd**)					
	EMTO		**MTO**		**SO**	
	RMSe	**Bias**	**RMSe**	**Bias**	**RMSe**	**Bias**
LAT thor.*	27.86 ± 21.16	0.86 ± 6.96	194.61 ± 4.11	-71.14 ± 1.63	181.74 ± 8.50	-59.43 ± 41.57
LAT lum.*	9.52 ± 2.93	3.43 ± 15.69	74.59 ± 2.81	-28.48 ± 4.54	81.07 ± 2.95	15.82 ± 99.31
LAT ili.*	10.09 ± 2.91	2.38 ± 16.72	39.02 ± 1.39	-46.07 ± 7.75	65.68 ± 9.05	-30.84 ± 51.43
TRI long	17.13 ± 8.48	7.94 ± 22.05	91.30 ± 3.40	-90.48 ± 4.51	115.88 ± 7.98	-87.84 ± 47.96
TRI lat.*	7.50 ± 1.06	8.41 ± 26.32	71.46 ± 0.62	-84.38 ± 10.52	76.31 ± 2.33	-6.28 ± 122.86
TRI med.*	13.69 ± 18.98	-5.61 ± 27.22	106.37 ± 5.56	-185.10 ± 10.31	107.50 ± 4.04	-108.40 ± 127.85
BRA*	16.07 ± 3.58	1.43 ± 7.86	30.03 ± 1.68	-71.83 ± 5.37	115.12 ± 17.00	-45.21 ± 61.99
PEC clav.*	18.89 ± 4.18	1.38 ± 6.54	51.31 ± 2.36	-12.64 ± 1.95	68.82 ± 4.24	8.40 ± 61.53
PEC ster.*	23.34 ± 7.20	3.07 ± 8.18	193.48 ± 5.94	-20.92 ± 4.96	189.23 ± 5.61	-6.50 ± 54.52
PEC ribs*	17.73 ± 21.00	0.77 ± 11.94	126.77 ± 3.93	-65.48 ± 4.62	129.92 ± 6.12	-11.86 ± 90.24
DELT ant.	21.57 ± 22.98	0.63 ± 34.19	126.40 ± 3.04	-359.26 ± 23.48	158.74 ± 13.48	-232.20 ± 221.08
DELT mid.*	9.09 ± 1.46	6.19 ± 20.29	16.35 ± 0.50	-82.13 ± 7.24	65.16 ± 8.26	-69.15 ± 47.97
DELT pos.*	37.13 ± 17.91	2.94 ± 20.00	371.91 ± 9.91	-191.04 ± 11.81	334.00 ± 19.27	-178.42 ± 51.41
SUP*	22.15 ± 5.30	1.95 ± 17.25	176.15 ± 4.89	-171.19 ± 11.43	168.57 ± 5.46	-55.60 ± 150.79
INF*	62.11 ± 39.07	16.53 ± 56.31	450.31 ± 13.52	-388.01 ± 28.98	381.16 ± 16.50	-195.68 ± 245.07
SUB	32.49 ± 7.37	10.94 ± 29.54	37.40 ± 3.23	-29.72 ± 14.76	260.64 ± 39.33	35.07 ± 220.35
BIC long*	28.58 ± 8.08	-0.49 ± 21.65	225.32 ± 12.11	-216.96 ± 21.30	242.76 ± 9.89	-137.01 ± 187.65
BIC short*	21.03 ± 8.46	0.70 ± 15.97	80.78 ± 1.94	-60.58 ± 9.12	120.27 ± 7.40	-45.55 ± 93.70
TRA up1	4.22 ± 0.69	1.88 ± 3.40	3.36 ± 0.13	-1.54 ± 0.64	35.61 ± 4.30	8.88 ± 32.92
TRA up2	7.54 ± 1.22	-0.36 ± 5.28	17.44 ± 0.67	-15.04 ± 2.09	64.80 ± 6.53	23.07 ± 57.60
MEAN(mean) ± SD(mean)	**20.39 ± 13.24**	**3.25 ± 4.78**	**124.22 ± 118.22**	**-109.60 ± 110.35**	**148.15 ± 94.01**	**-58.94 ± 76.66**

Table 4 RMSe and bias between the noise-free reference and estimated muscle activations with high co-contraction (n = 30 trials), for the 20 lines of action of the model. *Note.* A positive bias corresponds to an overestimation.

Muscle lines of action	**Activations** (unitless) (**mean ± sd**)					
	EMTO		**MTO**		**SO**	
	RMSe	**Bias**	**RMSe**	**Bias**	**RMSe**	**Bias**
LAT thor.	0.11 ± 0.04	0.00 ± 0.03	0.49 ± 0.01	-0.24 ± 0.16	0.46 ± 0.02	-0.24 ± 0.16
LAT lum.	0.07 ± 0.01	0.01 ± 0.02	0.36 ± 0.01	0.02 ± 0.12	0.39 ± 0.01	0.02 ± 0.12
LAT ili.	0.06 ± 0.01	0.01 ± 0.03	0.13 ± 0.01	-0.05 ± 0.09	0.21 ± 0.03	-0.05 ± 0.09
TRI long	0.10 ± 0.02	0.06 ± 0.09	0.26 ± 0.01	-0.31 ± 0.19	0.33 ± 0.02	-0.31 ± 0.19
TRI lat.	0.04 ± 0.00	0.05 ± 0.08	0.29 ± 0.00	-0.00 ± 0.36	0.30 ± 0.01	-0.00 ± 0.36
TRI med.	0.09 ± 0.07	-0.01 ± 0.07	0.39 ± 0.02	-0.28 ± 0.32	0.40 ± 0.02	-0.28 ± 0.32
BRA	0.02 ± 0.00	0.01 ± 0.04	0.04 ± 0.00	-0.23 ± 0.29	0.15 ± 0.02	-0.23 ± 0.29
PEC clav.	0.04 ± 0.01	0.02 ± 0.03	0.08 ± 0.00	0.05 ± 0.28	0.11 ± 0.01	0.05 ± 0.28
PEC ster.	0.05 ± 0.01	0.02 ± 0.03	0.32 ± 0.01	-0.02 ± 0.17	0.31 ± 0.01	-0.02 ± 0.17
PEC ribs	0.12 ± 0.08	0.03 ± 0.04	0.48 ± 0.02	-0.02 ± 0.26	0.49 ± 0.02	-0.02 ± 0.26
DELT ant.	0.10 ± 0.07	0.01 ± 0.03	0.36 ± 0.01	-0.23 ± 0.21	0.47 ± 0.04	-0.23 ± 0.21
DELT mid.	0.06 ± 0.01	0.05 ± 0.08	0.07 ± 0.00	-0.24 ± 0.19	0.30 ± 0.04	-0.24 ± 0.19
DELT pos.	0.05 ± 0.01	0.01 ± 0.03	0.36 ± 0.01	-0.29 ± 0.09	0.33 ± 0.02	-0.29 ± 0.09
SUP	0.09 ± 0.01	0.01 ± 0.04	0.38 ± 0.01	-0.12 ± 0.32	0.36 ± 0.01	-0.12 ± 0.32
INF	0.09 ± 0.03	0.03 ± 0.05	0.43 ± 0.01	-0.18 ± 0.25	0.37 ± 0.02	-0.18 ± 0.25
SUB	0.03 ± 0.01	0.01 ± 0.02	0.02 ± 0.00	0.03 ± 0.16	0.19 ± 0.03	0.03 ± 0.16
BIC long	0.08 ± 0.01	0.01 ± 0.03	0.36 ± 0.02	-0.22 ± 0.30	0.39 ± 0.02	-0.22 ± 0.30
BIC short	0.08 ± 0.01	0.01 ± 0.04	0.18 ± 0.00	-0.10 ± 0.22	0.28 ± 0.02	-0.10 ± 0.22
TRA up1	0.05 ± 0.01	0.02 ± 0.03	0.03 ± 0.00	0.08 ± 0.28	0.30 ± 0.04	0.08 ± 0.28
TRA up2	0.07 ± 0.01	0.02 ± 0.03	0.09 ± 0.00	0.16 ± 0.35	0.40 ± 0.04	0.16 ± 0.35
MEAN(mean) ± SD(mean)	**0.07 ± 0.03**	**0.02 ± 0.02**	**0.26 ± 0.16**	**-0.11 ± 0.14**	**0.33 ± 0.10**	**-0.11 ± 0.14**

Table 5 RMSe and bias in degree between the noise-free reference and estimated DOFs of the model with low co-contraction. *Note.* GH: glenohumeral; SD: standard deviation

DOFs	**Angles (°) (mean ± sd)**					
	EMTO		**MTO**		**SO**	
	RMSe	**Bias**	**RMSe**	**Bias**	**RMSe**	**Bias**
Clavicular rotation	1.52 ± 0.29	0.18 ± 1.51	1.98 ± 0.43	0.78 ± 1.82	1.14 ± 0.08	-0.05 ± 1.12
Scapular tilting	1.71 ± 0.25	-0.16 ± 1.64	2.18 ± 0.48	-0.87 ± 1.98	1.28 ± 0.09	0.06 ± 1.25
GH flexion	0.63 ± 0.11	0.03 ± 0.58	0.76 ± 0.22	-0.08 ± 0.75	0.36 ± 0.03	0.01 ± 0.35
GH abduction	0.97 ± 0.13	-0.14 ± 0.89	1.18 ± 0.33	0.09 ± 1.18	0.55 ± 0.06	-0.01 ± 0.53
GH axial rotation	1.49 ± 0.49	-0.06 ± 1.36	1.54 ± 0.47	0.17 ± 1.51	0.88 ± 0.11	0.02 ± 0.79
Elbow flexion	0.90 ± 0.39	0.16 ± 0.93	0.88 ± 0.48	-0.05 ± 0.97	0.48 ± 0.04	0.01 ± 0.45
MEAN(mean) ± SD(mean)	**1.20 ± 0.43**	**0.00 ± 0.15**	**1.42 ± 0.58**	**0.01 ± 0.53**	**0.78 ± 0.37**	**0.00 ± 0.04**

Table 6 RMSe and bias between the noise-free reference and estimated muscle forces with low co-contraction (n = 30 trials) for the 20 lines of action of the model.

Note. A positive bias corresponds to an overestimation. An asterisk was added next to the muscle lines of action for which a significant *Optimisation method* effect was observed on **Fig. 8**.

Muscle lines of action	**Forces** (N) (**mean ± sd**)					
	EMTO		**MTO**		**SO**	
	RMSe	**Bias**	**RMSe**	**Bias**	**RMSe**	**Bias**
LAT thor.	6.27 ± 0.90	1.60 ± 3.11	44.55 ± 5.68	-8.39 ± 1.83	138.45 ± 9.76	3.11 ± 42.22
LAT lum.	5.74 ± 0.45	0.55 ± 7.54	19.26 ± 2.61	-27.21 ± 7.18	60.78 ± 7.54	21.72 ± 110.97
LAT ili.	4.06 ± 0.70	1.81 ± 7.47	16.18 ± 1.42	-21.89 ± 8.93	65.71 ± 10.49	-9.31 ± 51.48
TRI long	3.96 ± 0.61	1.80 ± 3.02	21.61 ± 2.53	-14.40 ± 3.27	101.89 ± 10.61	-10.41 ± 49.35
TRI lat.*	3.50 ± 0.68	4.28 ± 4.62	8.72 ± 0.74	-29.98 ± 9.72	44.78 ± 11.57	53.30 ± 124.69
TRI med.*	5.47 ± 0.62	0.79 ± 5.83	20.92 ± 1.69	-37.62 ± 12.22	53.86 ± 7.66	35.85 ± 129.15
BRA	7.82 ± 1.45	-0.81 ± 2.80	29.45 ± 2.90	-12.16 ± 6.60	123.71 ± 30.57	5.12 ± 57.18
PEC clav.*	8.47 ± 1.61	0.32 ± 3.09	26.06 ± 3.40	-6.52 ± 3.18	60.23 ± 5.99	14.38 ± 63.63
PEC ster.	8.22 ± 1.49	1.59 ± 3.63	25.72 ± 2.82	-9.88 ± 5.00	58.91 ± 5.68	8.84 ± 56.89
PEC ribs	3.66 ± 0.54	-0.04 ± 3.87	20.51 ± 1.20	-19.02 ± 4.21	55.54 ± 7.69	35.11 ± 92.19
DELT ant.	6.66 ± 1.09	4.48 ± 11.00	50.29 ± 3.47	-69.48 ± 23.31	146.59 ± 9.87	53.88 ± 222.99
DELT mid.	3.86 ± 0.56	0.91 ± 3.14	8.98 ± 0.66	-15.95 ± 5.29	66.97 ± 10.03	-0.52 ± 49.78
DELT pos.	15.35 ± 2.10	1.67 ± 7.32	82.38 ± 5.81	-21.67 ± 8.36	234.53 ± 28.28	-9.43 ± 50.78
SUP	8.63 ± 1.31	-1.09 ± 6.99	52.72 ± 6.92	-37.32 ± 13.27	167.81 ± 13.54	67.20 ± 149.24
INF*	18.63 ± 3.12	10.09 ± 13.93	119.29 ± 10.46	-102.88 ± 29.85	271.19 ± 23.26	88.10 ± 250.23
SUB	17.61 ± 3.75	7.41 ± 15.88	37.05 ± 5.04	-28.26 ± 20.38	270.61 ± 37.41	44.30 ± 226.94
BIC long	12.01 ± 1.47	0.17 ± 8.74	77.06 ± 10.80	-69.67 ± 22.04	193.30 ± 13.04	-0.17 ± 187.93
BIC short	7.64 ± 0.99	2.59 ± 5.38	23.62 ± 2.14	-9.72 ± 8.83	95.61 ± 15.82	4.63 ± 89.85
TRA up1	1.91 ± 0.35	0.56 ± 1.62	2.22 ± 0.24	-1.33 ± 1.00	34.18 ± 4.11	7.71 ± 32.38
TRA up2	2.68 ± 0.46	0.46 ± 2.39	7.66 ± 0.87	-5.70 ± 3.65	65.54 ± 4.76	29.04 ± 56.58
MEAN(mean) ± SD(mean)	**7.61 ± 4.83**	**1.96 ± 2.75**	**34.71 ± 29.44**	**-27.45 ± 25.85**	**115.51 ± 75.74**	**22.12 ± 27.83**

Table 7 RMSe and bias between the noise-free reference and estimated muscle activations with low co-contraction (n = 30 trials), for the 20 lines of action of the model. *Note.* A positive bias corresponds to an overestimation.

Muscle lines of action	**Activations** (unitless) (**mean ± sd**)					
	EMTO		**MTO**		**SO**	
	RMSe	**Bias**	**RMSe**	**Bias**	**RMSe**	**Bias**
LAT thor.	0.04 ± 0.00	0.01 ± 0.01	0.12 ± 0.02	-0.03 ± 0.01	0.35 ± 0.02	0.01 ± 0.16
LAT lum.	0.05 ± 0.00	0.00 ± 0.01	0.09 ± 0.01	-0.03 ± 0.01	0.29 ± 0.03	0.03 ± 0.14
LAT ili.	0.02 ± 0.00	0.00 ± 0.01	0.05 ± 0.00	-0.04 ± 0.01	0.21 ± 0.03	-0.02 ± 0.09
TRI long	0.03 ± 0.00	0.02 ± 0.01	0.05 ± 0.01	-0.05 ± 0.01	0.29 ± 0.03	-0.04 ± 0.19
TRI lat.	0.01 ± 0.00	0.03 ± 0.01	0.04 ± 0.00	-0.07 ± 0.03	0.17 ± 0.04	0.16 ± 0.37
TRI med.	0.04 ± 0.00	0.01 ± 0.02	0.07 ± 0.01	-0.10 ± 0.03	0.21 ± 0.03	0.08 ± 0.33
BRA	0.01 ± 0.00	0.01 ± 0.01	0.04 ± 0.00	-0.05 ± 0.03	0.16 ± 0.04	0.02 ± 0.27
PEC clav.	0.02 ± 0.00	0.01 ± 0.01	0.04 ± 0.01	-0.03 ± 0.02	0.10 ± 0.01	0.07 ± 0.29
PEC ster.	0.02 ± 0.00	0.01 ± 0.01	0.04 ± 0.00	-0.03 ± 0.02	0.10 ± 0.01	0.03 ± 0.18
PEC ribs	0.03 ± 0.00	0.01 ± 0.01	0.08 ± 0.00	-0.05 ± 0.01	0.22 ± 0.03	0.11 ± 0.26
DELT ant.	0.04 ± 0.00	0.01 ± 0.01	0.15 ± 0.01	-0.06 ± 0.02	0.44 ± 0.03	0.06 ± 0.22
DELT mid.	0.03 ± 0.00	0.02 ± 0.01	0.04 ± 0.00	-0.05 ± 0.02	0.30 ± 0.04	0.01 ± 0.19
DELT pos.	0.03 ± 0.00	0.00 ± 0.01	0.08 ± 0.01	-0.04 ± 0.01	0.23 ± 0.03	-0.02 ± 0.08
SUP	0.04 ± 0.00	0.00 ± 0.02	0.11 ± 0.01	-0.07 ± 0.03	0.36 ± 0.03	0.14 ± 0.31
INF	0.03 ± 0.00	0.02 ± 0.01	0.12 ± 0.01	-0.10 ± 0.03	0.28 ± 0.02	0.09 ± 0.26
SUB	0.01 ± 0.00	0.01 ± 0.01	0.03 ± 0.00	-0.02 ± 0.02	0.20 ± 0.03	0.03 ± 0.17
BIC long	0.05 ± 0.00	0.01 ± 0.01	0.12 ± 0.02	-0.11 ± 0.04	0.31 ± 0.02	-0.00 ± 0.30
BIC short	0.03 ± 0.00	0.02 ± 0.01	0.05 ± 0.01	-0.01 ± 0.02	0.22 ± 0.04	0.02 ± 0.21
TRA up1	0.02 ± 0.00	0.01 ± 0.01	0.02 ± 0.00	-0.01 ± 0.01	0.29 ± 0.04	0.07 ± 0.28
TRA up2	0.03 ± 0.00	0.01 ± 0.01	0.04 ± 0.00	-0.03 ± 0.02	0.40 ± 0.03	0.18 ± 0.34
MEAN(mean) ± SD(mean)	**0.03 ± 0.01**	**0.01 ± 0.01**	**0.07 ± 0.04**	**-0.05 ± 0.03**	**0.26 ± 0.09**	**0.05 ± 0.06**